Check for updates

Energy Technology
Generation, Conversion, Storage, Distribution
www.entechnol.de

Representativeness of Energy Rating acc. to IEC 61853 for Different Locations in Middle and South Europe

Mariella Rivera, Christian Reise, and Ulli Kräling*

The energy rating standard series IEC 61 853 parts 1–4 provide a procedure to calculate the performance of a photovoltaic (PV) module for six different reference climates. The results, denoted as climate specific energy rating (CSER), aim to predict the module's energy output for a complete year under maximum power point operation. The reference climate profiles shall represent the typical operating conditions of a PV module in a given region. Our study investigates the representativeness of these reference climates profiles for several locations in South and Central Europe. We gathered both ground- and satellite-based data sets from different weather monitoring stations. Using such data for our specific location in Freiburg, Germany, and a specific reference module, we found deviations ranging from 2.0% to 2.9% compared to the CSER using the *temperate continental* profile. Further, we analyze the annual impact of the loss factors: reflectivity as function of angle of incidence, solar spectrum, ambient temperature, and irradiance on module performance. For an in-depth PV module benchmarking, we recommend the use of site-specific meteorological data for an accurate module performance assessment, rather than relying on the more general estimates from the standard procedure, which do not intend to capture site-specific effects.

1. Introduction

As a means of evaluating and comparing the performance of PV modules, their nominal power is measured under standard test conditions (STC: 1000 W m^{-2}, 25 °C, AM1.5). However, this approach fails to accurately represent the behavior of PV modules in real conditions. Whereas energy yield predictions, which consider installation conditions and use site-specific meteorological data, provide a more accurate assessment of the module's performance. However, data sheets often do not contain sufficient information for a proper parameterization of the yield models utilized for such predictions.

To address this issue, the IEC-61 853 standard provides a procedure for calculating module performance under different, preestablished climate conditions, with assumptions about operating and installation conditions (such as tilt and orientation). During the calculation, various parameters that reduce the effective irradiance reaching the PV module are taken into account, including (i) the surface reflectivity when light reaches at angles of incidence (AOI) different from perpendicular to the surface, (ii) the variations in solar spectrum and the spectral response (SR) of the device, (iii) the module temperature (modeled as a function of irradiance, ambient temperature, and wind speed), and (iv) the irradiance level.[1–3]

By providing a standardized procedure for calculating module performance, IEC-61 853 enables a more accurate and consistent comparisons between different PV modules. The standard follows an energy rating (ER) methodology, using the performance indicator known as the climate-specific energy rating (CSER), equivalent to the module's direct current performance ratio (PRDC). The CSER is a ratio between the energy produced by the module over a year of irradiation under a specific climate condition specified by the standard and the energy that the module would have been produced if it was operating under STC.

$$\mathrm{CSER} = \frac{E_{\mathrm{mod,year}}\, G_{\mathrm{STC}}}{P_{\mathrm{max,STC}}\, H_{\mathrm{p}}} \tag{1}$$

where H_{p} is the total global irradiance in-plane of array (POA) for the standard climate period (1 year) provided by part 4 of the standard,[4] G_{STC} is the irradiance at STC, $P_{\mathrm{max,STC}}$ is the maximum or nominal power under STC, and $E_{\mathrm{mod,year}}$ is the energy produced by the module over the year. The ER methodology has two main inputs, as shown in **Figure 1**.

1.1. PV Module Data

The module's performance is determined under controlled specific conditions, whether through indoor or outdoor procedures.[5,6] During this process, the module's angular and spectral responses are determined, as well as the coefficients for calculating its temperature. A power matrix is also generated, which

M. Rivera, C. Reise, U. Kräling
Analysis, PV Modules, and Power Plants
Fraunhofer Institute for Solar Energy Systems ISE
Heidenhofstr. 2, 79110 Freiburg, Germany
E-mail: mariella.josefina.rivera.aguilar@ise.fraunhofer.de

The ORCID identification number(s) for the author(s) of this article can be found under https://doi.org/10.1002/ente.202300356.

© 2023 The Authors. Energy Technology published by Wiley-VCH GmbH. This is an open access article under the terms of the Creative Commons Attribution License, which permits use, distribution and reproduction in any medium, provided the original work is properly cited.

DOI: 10.1002/ente.202300356

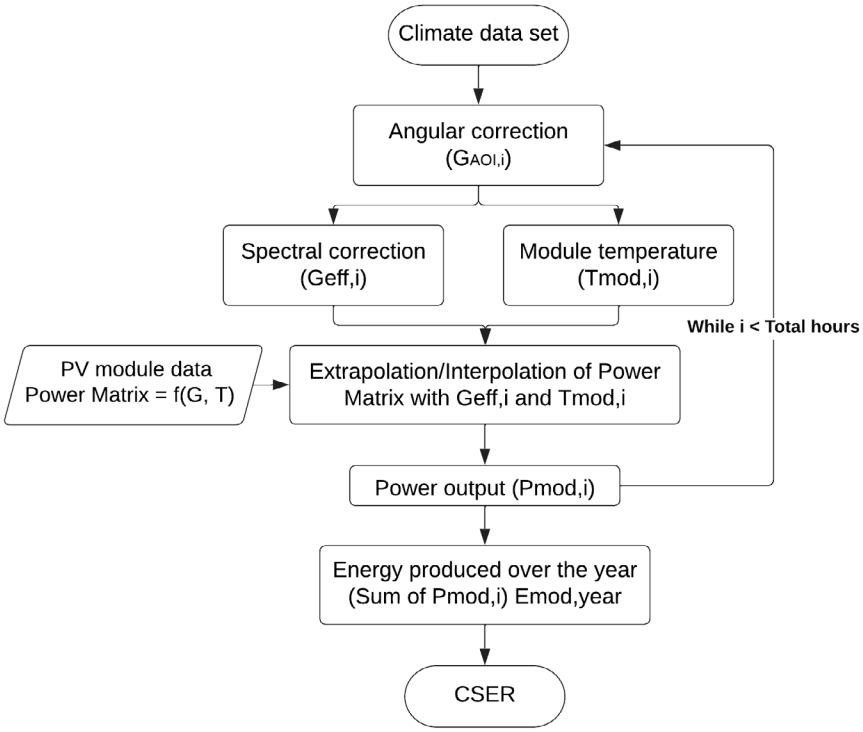

Figure 1. Standard procedure given by IEC 61 853-3 for the calculation of CSER.

includes the module's power output under different levels of irradiance and temperature.

1.2. Climate Data Sets

The module's performance is simulated using satellite-based climate data from six different regions around the world: tropical humid, subtropical arid (desert), subtropical coastal, temperate coastal, high elevation (above 3000 m), and temperate continental.[4] After correcting the effective irradiance and modeling the module temperature, the module's performance is interpolated or extrapolated from its power matrix to the specific conditions of each of these climate profiles.

The aim of this study is to assess the representativeness of standard climate profiles for specific locations by incorporating site-specific climate profiles to calculate the site-specific energy rating (SSER). We then compare the SSER with the standard location's climate-specific energy rating (CSER). Previous studies have suggested the use of specific climate data sets for Europe and presented various profiles to describe the conditions in Europe, which have been shown to accurately capture differences in module performance.[1,7]

Additionally, the study also focuses on the differences between satellite-derived and ground-based climate data, specifically the spectral irradiance measurements, and how they affect the CSER. Previous studies have already found good agreement between these two types of data, despite the more detailed representation of atmospheric parameters with ground-based data.[8,9]

This study aims to contribute to the research of factors that have the most significant and variable impact on the ER under standard and specific climate profiles.[1,2,10–12] Monocrystalline silicon PV modules from highly efficient technologies (PERC, HJT, and IBC) are compared under different conditions of ambient temperature, irradiance levels, and angular and spectral effects. We emphasize that a more detailed and site-specific assessment of PV modules, rather than relying solely on a performance indicator, is crucial for informed decision-making in the selection of PV modules for investment and technology benchmarking purposes.

2. Methodology

The parameters given in the standard climate profiles for the ER calculations are broadband irradiance (horizontal and in POA at a 20° tilt angle), ambient temperature, wind speed, and spectrally resolved irradiance in POA (in a set of 29 wavelength bands—"Kato-bands" ranging from 306.8 to 4605.65 nm). These parameters are given as hourly values for a period of one year.

With the aim to calculate the SSER, different weather monitoring stations operated by Fraunhofer ISE are used. We also include a central Europe data set with coordinates 48°N, 12°E (Munich) provided by Ref. [1]. This reference climate profile is near one of our monitoring stations in Freiburg, Germany (48°N, 7.8°E). The before mentioned locations, regarding weather conditions should be represented by the *temperate continental* profile. We further include a location in Negev, Israel (30.6°N, 34.8°E), which due to its desert conditions should be represented by the *subtropical arid* profile; and a location in Gran Canaria, Spain (27.8°N, 15.4°W) represented by the *subtropical coastal* profile.

© 2023 The Authors. Energy Technology published by Wiley-VCH GmbH

21944296, 0, Downloaded from https://onlinelibrary.wiley.com/doi/10.1002/ente.202300356 by Fraunhofer Ise Inst. Solar Energy Systems, Wiley Online Library on [20/11/2023]. See the Terms and Conditions (https://onlinelibrary.wiley.com/terms-and-conditions) on Wiley Online Library for rules of use; OA articles are governed by the applicable Creative Commons License

21944296, 0, Downloaded from https://onlinelibrary.wiley.com/doi/10.1002/ente.202300356 by Fraunhofer Ise Inst. Solar Energy Systems, Wiley Online Library on [20/11/2023]. See the Terms and Conditions (https://onlinelibrary.wiley.com/terms-and-conditions) on Wiley Online Library for rules of use; OA articles are governed by the applicable Creative Commons License

2.1. Ground-Based Data

Fraunhofer ISE's monitoring stations are equipped with weather sensors for ambient temperature and wind speed, as well as broadband irradiance sensors positioned horizontally or tilted between 20° and 30°, depending on the location. However, data availability may vary depending on the selected years. To ensure data consistency, broadband irradiance values in horizontal position are extracted from the stations and transposed to POA based on available data, following the procedure:[13] 1) Direct normal irradiance (DNI) modeled based on clear sky conditions, global and diffuse horizontal irradiance (GHI and DHI);[13] 2) Direct irradiance in POA (Beam) calculated using the AOI.

$$\text{Beam} = \text{DNI}\cos(\text{AOI}) \tag{2}$$

3) Diffuse irradiance in POA (D_{POA}) as the sum of the sky (*Dsky*) and ground reflected (*Dground*) components, according to Klucher model, using GHI and DHI:[14] i) For the Gran Canaria station, DHI was missing, so it was simulated based on Erbs model;[15] 4) Global irradiance in POA (G_{POA}) modeled based on the availability of data: i) For broadband and spectral irradiance available only in horizontal plane, the G_{POA} is calculated from the sum of the direct and diffuse irradiance components in POA, from previous steps.

$$G_{\text{POA}} = \text{Beam} + D_{\text{POA}} \tag{3}$$

ii) For spectral irradiance available in POA, G_{POA} is calculated as the integration of spectral irradiance ($G_{\lambda-\text{POA}}$) values through all the wavelength bands.

$$G_{\text{POA}} = \sum_{\lambda} G_{\lambda-\text{POA}} \tag{4}$$

The availability and format of data for spectral irradiance measurements vary across our stations (**Table 1**). For one of the monitoring stations in Freiburg (year 2020), spectral irradiance data are available from a sensor in horizontal position. Therefore, a simplified normalization factor is calculated using the POA broadband irradiance modeled at a 20° tilt angle. This enables transposition of spectral irradiance data from any angle to 20°, as shown in Equation (5) and (6).

$$N_{\text{factor}j} = \frac{G_{\text{jPOA}-20^\circ}}{\sum_{\lambda} G_{\lambda}^{j}} \tag{5}$$

Table 1. Site-specific locations, type of spectroradiometer and its wavelength range. The inclination angle of the sensor and year of data collection.

Site	Sensors	Wavelength range [nm]	Tilt angle [°]	Year
Freiburg	EKO MS710- MS712	300–1700	29	2014
Freiburg	EKO MS710- MS712	300–1700	0	2020
Gran Canaria	EKO MS711	300–1100	23	2018
Negev	EKO MS711	300–1100	23	2020

$$G_{\lambda-20^\circ}^{j} = N_{\text{factor}j} \times G_{\lambda}^{j} \tag{6}$$

Here, $G_{\text{jPOA}-20^\circ}$ is the broadband irradiance at 20° tilt angle for each time step j, and $\sum_{\lambda} G_{\lambda}^{j}$ is the sum of spectral irradiance across all wavelength bands for a given time step. The normalization factor $N_{\text{factor}j}$ can be applied to all wavelength bands for each time step ($G_{\lambda-20^\circ}^{j}$). It is important to note that this procedure assumes the transposition factor will be the same for each wavelength band. It is worth mentioning that the other monitoring stations are used with their unmodified tilt angles. Only the Freiburg (2020) data set employs this simplified normalization factor.

2.2. Satellite-Based Data

Our "satellite-based" climate profiles are a combination of ground- and satellite-based data. The ambient temperature and wind speed data are ground-based, while the broadband and spectral irradiance are obtained from the German Weather Service (Deutscher Wetterdienst—DWD) through their EUMETSAT's Satellite Application Facility on Climate Monitoring (CM SAF).[16] The irradiance data comprises DNI and GHI in 32 wavelength bands ranging from 240 to 4606 nm. For consistency with the IEC-61 853 data sets, the first three bands are removed, resulting in 29 bands ranging from 307 to 4606 nm. The data processing and calculation of $G_{\lambda-\text{POA}}$ for each band is done as follows: 1) DHI is calculated as a function of DNI and GHI using Equation (7).

$$\text{DHI} = \text{GHI} - \text{DNI}\cos(\text{solar zenith}) \tag{7}$$

2) The Beam is calculated from DNI using Equation (2); 3) The reflected irradiance (D_{POA}) from ground and sky is calculated using the Klucher model.;[14] 4) The sum of POA components is applied to each band to calculate ($G_{\lambda-\text{POA}}$) using Equation (3); 5) Finally, G_{POA} is calculated using Equation (4).

2.3. Energy Rating Calculation

For the ER calculation, this study adopts the methodology presented in Ref. [17], which has been validated through a Round Robin study to reduce ambiguities in certain steps of the standard procedure. The implementation tools from Ref. [18] are used as a reference for the numerical treatment of the spectral correction and power matrix extrapolation (Figure 1).

Furthermore, we modify the spectral correction for calculation of the effective irradiance (G_{eff}) to account for the narrower wavelength range from our monitoring stations (ground-based data). The standard approach uses the spectral mismatch factor (SMM) with integration limits from 300 to 4000 nm.[19] However, since our ground-based spectral irradiance ranges only up to 1100 or 1700 nm, we transform it into 29 "Kato bands" following the procedure in Ref. [17]. We then integrate within the respective band's limits, based on the equation for SMM from IEC 60 904-7[20,21]

© 2023 The Authors. Energy Technology published by Wiley-VCH GmbH

$$\mathrm{SMM} = \frac{\int_a^b \mathrm{SRref}(\lambda)\mathrm{Eref}(\lambda)d\lambda \times \int_a^b \mathrm{SRmodule}(\lambda)\,\mathrm{Emeas}(\lambda)d\lambda}{\int_a^b \mathrm{SRref}(\lambda)\mathrm{Emeas}(\lambda)d\lambda \times \int_a^b \mathrm{SRmodule}(\lambda)\,\mathrm{Eref}(\lambda)d\lambda} \tag{8}$$

$$G_{\mathrm{eff}} = \mathrm{SMM} \times G_{\mathrm{AOI}} \tag{9}$$

where the wavelength limits a and b used for the integration are based on the wavelength range of our spectroradiometers and are chosen from the 29 "Kato bands" (a= 306.8...327.8 nm, b= 1045.7...1194.2 nm or 1613.5...1964.8 nm depending on the maximum wavelength limit of the spectrometer used). The SRmodule(λ) is the spectral response of the PV modules, and SRref(λ) is the spectral response of the pyranometer (considered unity for all wavelengths, SRref = 1). Emeas(λ) is the measured spectral irradiance, and Eref(λ) is the reference spectrum.[22] It is important to note that the integration range should cover the sensitivity of the PV module.

2.4. Reference PV Module Data

For our comparison of standard versus site-specific climate profiles starting in the next section, we use reference data set for a crystalline silicon PV module provided by a Round Robin study that contains the module's intrinsic angular and thermal coefficients, SR, and Power Matrix.[17] These data are necessary for the angular and spectral correction, module temperature calculation, and the power output extrapolation. The Round Robin study also shows the CSER results for their reference PV module in the six standard climate profiles, where all participants agree with deviations lower than 0.1%. This allows us to compare our implementation of the methodology with theirs, and we have achieved minimal deviations (0.085%).

3. CSER versus SSER

In this initial stage of results analysis, the focus is on comparing the performance of the reference PV module in site-specific locations, calculating SSER, and its performance on a representative standard climate profile, calculating CSER. Furthermore, to understand the specific parameters that influence the ER, we calculate the gains and losses in converted irradiance, which are directly correlated to performance variations. The factors that cause these effects include reflectivity due to different AOI, variations in the solar spectrum, ambient temperature, and irradiance levels.[1,2] Additionally, the study considers any variations that may occur between satellite- and ground-based data, particularly in the case of data collected in Freiburg.

As first result for this standard module, the SSER for Freiburg ranges from 94.6% to 95.5% across the four available meteorological data sets, with a standard deviation of 0.38%. Using the *temperate continental* data set from the standard leads to a higher CSER of 97.5%. When comparing the results for Freiburg to the standard, the deviations range from 1.96% to 2.94%, with Freiburg underpredicting the standard. For Munich, the deviation from the standard is –2.55% (**Figure 2**). For Gran Canaria, the SSER is compared to the *subtropical coastal* data set, resulting in a deviation of 1.65% underpredicting the standard. For Negev, when compared to the *subtropical arid* profile, the SSER results in an overprediction of 1.05% (**Table 2**).

3.1. Angle of Incidence Effect

The reflectivity of a PV module usually increases when solar radiation hits the surface at angles different from normal to the module's surface (AOI = 0°). To account for AOI effects, the standard considers the angular response of the module and corrects the global irradiance in POA.[19] To quantify the losses due to this effect, we use the irradiation for the entire year of data before and after angular correction, denoted as H_{year} and $H_{\mathrm{AOI,year}}$, respectively (Equation (10)).[1] This parameter accounts for the reflection losses depending not only on the sun's position but also on the proportion of diffuse irradiance and the module's tilt angle.

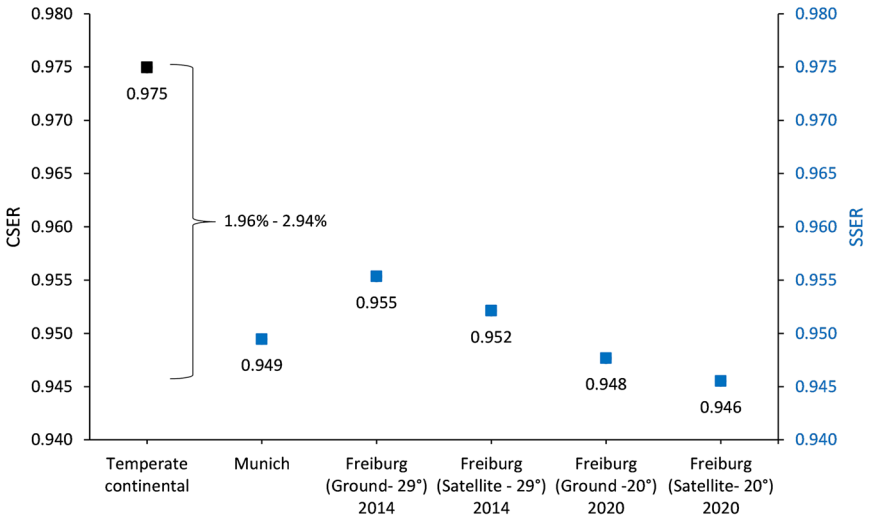

Figure 2. CSER for the reference PV module in the temperate continental profile and SSER for the specific locations in Munich and Freiburg, including the deviation range between standard and specific profiles.

© 2023 The Authors. Energy Technology published by Wiley-VCH GmbH

21944296, 0, Downloaded from https://onlinelibrary.wiley.com/doi/10.1002/ente.202300356 by Fraunhofer Ise inst. Solar Energy Systems, Wiley Online Library on [20/11/2023]. See the Terms and Conditions (https://onlinelibrary.wiley.com/terms-and-conditions) on Wiley Online Library for rules of use; OA articles are governed by the applicable Creative Commons License

21944296, 0, Downloaded from https://onlinelibrary.wiley.com/doi/10.1002/ente.202300356 by Fraunhofer Ise Inst. Solar Energy Systems, Wiley Online Library on [20/11/2023]. See the Terms and Conditions (https://onlinelibrary.wiley.com/terms-and-conditions) on Wiley Online Library for rules of use; OA articles are governed by the applicable Creative Commons License

Table 2. Comparison of CSER and SSER with their deviation (italic: CSER locations).

Location	CSER and SSER [%]	SSER deviation from CSER [%]
Temperate continental	97.5	
Munich	94.9	−2.55
Freiburg (Ground)—2014	95.5	−1.96
Freiburg (Satellite)—2014	95.2	−2.28
Freiburg (Ground)—2020	94.8	−2.73
Freiburg (Satellite)—2020	94.6	−2.94
Subtropical coastal	95.8	
Gran Canaria	94.1	−1.65
Subtropical arid (desert)	90.7	
Negev	91.7	+1.05

$$L_{\mathrm{AOI,year}} = \frac{H_{\mathrm{AOI,year}} - H_{\mathrm{year}}}{H_{\mathrm{year}}} \tag{10}$$

As shown in **Table 3**, the module's ER losses due to reflectivity as function of AOI range from −2.31% to −3.10% for temperate climate profiles. These results are very close to the range found by Ref. [1] for European sites. In ground-based data sets, the module tends to show higher losses than with satellite measurements (0.23% to 0.61% larger). For Freiburg, deviations with respect to the *temperate continental* profile seem to be larger than in Munich, with deviations ranging from −0.31% to +0.48%. The tendency is to have higher losses due to AOI when the proportion of diffuse irradiance is higher. As for Gran Canaria and Negev, they have bigger deviations from the standard profiles, especially Negev, where the module experiences higher losses than in the *subtropical arid* profile due to slightly higher AOI.

Table 3. Comparison of module's average annual gain or loss due to variations in the AOI ($L_{\mathrm{AOI,year}}$) for each climate profile, including the deviations of $L_{\mathrm{AOI,year}}$ for each specific location when compared to the standard climate profile (italic). Additionally, it presents the annual average irradiance weighted AOI and the proportion of diffuse irradiance (D_{POA}) in each climate.

Location	$L_{\mathrm{AOI,year}}$ [%]	Deviation [%]	Annual average weighted AOI [°]	Proportion of diffuse irradiance [%]
Temperate continental	−2.79		43.3	40.9
Munich	−2.63	+0.16	40.2	39.8
Freiburg (Ground)—2014	−3.10	−0.31	36.2	43.3
Freiburg (Satellite)—2014	−2.49	+0.30	36.7	43.1
Freiburg (Ground)—2020	−2.54	+0.25	38.7	40.3
Freiburg (Satellite)—2020	−2.31	+0.48	39.0	37.2
Subtropical coastal	−2.57		35.2	51.3
Gran Canaria	−1.96	+0.61	35.4	32.3
Subtropical arid (desert)	−2.10		36.6	26.5
Negev	−3.17	−1.07	38.2	27.8

3.2. Effect Due to Variation of Solar Spectrum

The energy conversion efficiency of a PV module depends on the spectrum of the incoming light. Typically, the performance of a module is measured under a defined spectrum (AM1.5).[22] However, in actual operating conditions, the sunlight spectrum differs from AM1.5, resulting in variations in module performance.[3] To account for these spectral effects, the standard IEC 61 853-3 calculates the effective irradiance (G_{eff}), which represents the actual values of incoming irradiance, using Equation (8) and (9). The effective irradiance is used to estimate the power output of the PV module. We quantify the gains and losses of incident irradiance due to spectrum variations using the effective yearly irradiation ($H_{\mathrm{eff,year}}$) and the yearly irradiation that considers angular dependencies ($H_{\mathrm{AOI,year}}$).[1]

$$L_{\mathrm{spec,year}} = \frac{H_{\mathrm{eff,year}} - H_{\mathrm{AOI,year}}}{H_{\mathrm{AOI,year}}} \tag{11}$$

In most of the locations, the reference PV module exhibits spectral gains, ranging from 1.55% to 3.37% for a temperate climate profile (**Table 4**). These results differ significantly from the results reported by Ref. [1] for Europe, where gains range from 0.3% to 1.8%. The differences in spectral gains between using satellite- and ground-based data range from 1.1% to 1.2%. For the data sets from Freiburg, there is a greater difference with the *temperate continental* profile in terms of spectral gains, ranging from −0.48% to 1.34%.

A larger deviation in the spectral effect is observed for Gran Canaria, which may be attributed to several factors. One possible explanation is the considerable differences in climate conditions, such as the proportion of diffuse irradiance, which was found to be 19% higher for *subtropical coastal* (Table 3). These differences need to be further validated with outdoor measurements, since the diffuse fraction has been modelled for Gran Canaria (Section 2.1) due to missing data in this study. The difference in atmospheric conditions could potentially cause a higher spectral mismatch, especially due to cloudiness as described in Ref. [23] and discussed in section "Ground- versus Satellite-based

Table 4. Comparison of module's average annual gain or loss due to variation in the solar spectrum ($L_{\mathrm{c,ear}}$) for each climate profile, including the deviations of the $L_{\mathrm{spec,year}}$ from the specific locations compared to the standard climate profiles (italic).

Location	$L_{\mathrm{spec,year}}$ [%]	Deviation [%]
Temperate continental	2.03	
Munich	1.93	−0.09
Freiburg (Ground)—2014	3.37	+1.34
Freiburg (Satellite) —2014	2.26	+0.24
Freiburg (Ground)—2020	2.79	+0.76
Freiburg (Satellite) —2020	1.55	−0.48
Subtropical coastal	3.29	
Gran Canaria	0.38	−2.91
Subtropical arid (desert)	0.63	
Negev	1.18	+0.55

© 2023 The Authors. Energy Technology published by Wiley-VCH GmbH

Spectral Irradiance" in the Supporting Information. Another contributing factor could be the shorter bandwidth of the spectroradiometer used in Gran Canaria. In this case, the true shape of the spectrum is lost due to the transformation carried out to convert the spectral irradiance from a limiting wavelength of 1100 nm into the 29 "Kato bands" format, which corresponds to a bandwidth limit of 1045.7...1194.2 nm.

The spectral mismatch (SMM) is used to quantify the energetic gain or loss in effective irradiance available to a PV module. When calculated for the entire year of available data and weighted with the irradiance (SMM_{year}), it is also equivalent to $1 + L_{spec,year}$. SMM compares the irradiance level detected by the module with that detected by a reference device (usually a pyranometer) under measured and reference conditions and expressing the difference as a ratio. SMM values lower than one indicate power loss (spectral losses) compared to the reference device, while values larger than one indicate power gains due to the spectral gains.[21]

In Freiburg, the annual average spectral irradiance for each Kato-band from the ground- and satellite-based data exhibits larger deviations (>2%) in the wavelength ranges of 306...407 nm, 684...742 nm, and 1613...2275 nm, while the deviations for the remaining bands are lower than 1.8%. Although average spectral irradiance values in each wavelength band are similar between types of data (Figure S1, Supporting Information), a more comprehensive overview of the differences can be obtained by analyzing the wavelength bands and SMM. The reference PV module's SMM shows a stronger seasonal variation for satellite-based data, with higher values in winter, where the differences between ground and satellite SMM values are smaller. The seasonal variation of SMM for ground-based data throughout the year is less than in the satellite-based climate profiles and in the standard profiles (which are satellite based as well) (**Figure 3**). More detail comparison can be found in Supporting Information (Ground- vs Satellite-based Spectral Irradiance)

3.3. Effect Due to Ambient Temperature

The effect of temperature on PV module performance is strong and determines most of the geographical variation.[1] In order to quantify the gain or loss in module efficiency due to the variation of module temperature, which differs from STC, we utilize an equation based on Ref. [2]

$$L_{T,year} = \frac{\sum_{i=0}^{N} G_i\,(\eta(G_{eff,i}, T_{mod,i}) - \eta(G_{eff,i}, T_{STC}))}{\sum_{i=0}^{N} G_{eff,i}\,\eta(G_{eff,i}, T_{STC})} \quad (12)$$

where $G_{eff,i}$ is the effective irradiance in each time step, N is the number of available time steps, T_{STC} is 25 °C, $T_{mod,i}$ is the module temperature, and η is the module efficiency at a specific irradiance and module temperature level.

Table 5 shows that in temperate climates, losses due to temperature variation range from −2.82% to −4.04%, except for the standard climate profile where the losses are rather small (−0.01%). This can be directly linked to the lower average operating ambient temperature in the latter case, with temperature differences to specific locations from 5.2 to 9.3 °C.

On the other hand, Negev and *subtropical arid* show significantly different losses, despite having a small temperature gap of only 1.7 °C. This indicates that for higher temperature values, the variability of losses due to temperature is higher, as shown in the correlation in Figure S4, Supporting Information.

3.4. Effect Due to Irradiance

We estimated the losses resulting from irradiance levels differing from STC (1000 W m^{-2}) by using the equation given in Ref. [2]. This equation is based on the module efficiency at STC and at different levels of effective irradiance.

$$L_{G,year} = \frac{\sum_{i=0}^{N} G_{eff,i}\,(\eta(G_{eff,i}, T_{STC}) - \eta_{STC})}{\sum_{i=0}^{N} G_{eff,i}\,\eta_{STC}} \quad (13)$$

The range of module's losses due to variations in irradiance levels is −1.30% to −1.69% for temperate climates, with a deviation from the standard profile of up to 0.39% (**Table 6**). The *temperate continental* profile shows an average daytime

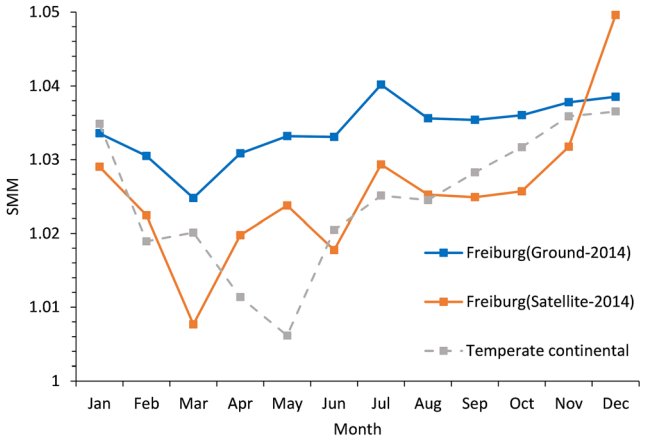

Figure 3. Monthly average SMM for ground- and satellite-based data sets of Freiburg (2014) and the standard climate temperate continental.

Table 5. Comparison of module's average annual gain or loss due to variation in temperature ($L_{T,year}$) for each climate profile, including the deviations of the $L_{T,year}$ from the specific locations compare to the standard climate profiles (italic). Additionally, it presents the annual irradiance-weighted ambient temperature.

Location	$L_{T,year}$ [%]	Deviation [%]	Annual irradiance weighted *Tamb* ($\Sigma Tamb \times G/\Sigma G$) [°C]
Temperate continental	−0.01		10.4
Munich	−2.82	−2.81	15.6
Freiburg (Ground) – 2014[a)]	−2.96	−2.95	19.0
Freiburg (Ground) – 2020[a)]	−4.04	−4.03	19.7
Subtropical coastal	−3.43		19.5
Gran Canaria	−3.33	+0.10	22.0
Subtropical arid (desert)	−7.28		23.4
Negev	−5.63	+1.65	25.1

[a)]The satellite-based locations are not included in this comparison since their ambient temperature is taken from ground measurements.

© 2023 The Authors. Energy Technology published by Wiley-VCH GmbH

21944296, 0, Downloaded from https://onlinelibrary.wiley.com/doi/10.1002/ente.202300356 by Fraunhofer Ise Inst. Solar Energy Systems, Wiley Online Library on [20/11/2023]. See the Terms and Conditions (https://onlinelibrary.wiley.com/terms-and-conditions) on Wiley Online Library for rules of use; OA articles are governed by the applicable Creative Commons License

Table 6. Comparison of module's average annual gain or loss due to variation of irradiance ($L_{G,year}$) for each climate profile, including the deviations of the $L_{G,year}$ from the specific locations compare to the standard climate profiles (italic). Additionally, it presents the annual average daytime operating irradiance and fraction of low irradiance.

Location	$L_{G,year}$ [%]	Deviation [%]	Average daytime operating irradiance ($\Sigma G^2/\Sigma G$) [W m^{-2}]	Fraction of low irradiance ($G_{POA} < 200$ W m^{-2}) [%]
Temperate continental	−1.69		555	11.1
Munich	−1.56	+0.13	605	12.0
Freiburg (Ground) - 2014	−1.71	−0.02	564	12.9
Freiburg (Satellite) - 2014	−1.49	+0.20	602	11.0
Freiburg (Ground) - 2020	−1.42	+0.27	631	10.3
Freiburg (Satellite) - 2020	−1.30	+0.39	625	8.6
Subtropical coastal	−1.43		644	10.5
Gran Canaria	−1.00	+0.44	630	5.5
Subtropical arid (desert)	−0.73		746	4.1
Negev	−0.78	−0.06	667	3.2

irradiance level significantly lower than most of the site-specific locations.

Module's losses due to irradiance deviate between ground- and satellite-based profiles by around 0.12% to 0.22%, with differences in their fraction of low irradiance ranging from 1.7% to 1.9%. The climates with the greatest losses are also the climates with the lowest average operating irradiance and a high fraction of low irradiance levels, such as *temperate continental*. For Gran Canaria and *subtropical coastal*, the loss differences are the largest (0.44%), which can be attributed to their differences in the amount of low irradiance levels throughout the year (a 5% difference).

From the previous analysis, it was found that the parameters that affect ER the most on a single reference PV module for climate profiles with temperate conditions are the ambient temperature (losses of 2.82% to 4.04%) and the AOI (losses of 2.31% to 3.10%). For Gran Canaria, the main differences with respect to the *subtropical coastal* profile come from solar spectrum variations, while Negev differs from *subtropical arid* mainly due to ambient temperature.

The comparison of ground- and satellite-based profiles (from Freiburg) shows that the biggest differences are due to the spectrum effect, followed by the AOI. The module in ground-based profiles has greater gains due to spectrum (1.1% to 1.2% larger) and larger losses due to AOI (0.23% to 0.61% larger).

4. Effect of PV Module Characteristics

To gain a more detailed understanding of how various PV module characteristics affect the ER, we conducted an analysis on a set of 11 monocrystalline silicon PV modules (c-Si) from different manufacturers and technologies (PERC, HJT, and IBC), with specifications provided in **Table 7**. The modules were first

Table 7. PV modules characteristic design parameters, maximum power (*Pmpp*) at STC, angular loss coefficient and temperature coefficient (TC).

Modules[a)]	Tech.[b)]	Cells[c)]	Module Size [m^2]	Pmpp @ STC [W]	I_{sc} @ STC [A]	V_{oc} @ STC [V]	Angular loss coeffiecient [a_r]	*TCPmpp* [% K^{-1}]
Mod_00[d)]	–	–	1.60	280.5	–	–	0.14571	−0.40
ModA_01	PERC	120 HC	1.84	377.2	11.44	42	0.12314	−0.33
ModB_02	PERC	60 FC	1.66	313.0	10.19	41	0.1439	−0.36
ModC_03	PERC	132 HC	1.89	380.5	10.68	45.03	0.10596	−0.34
ModD_04	PERC	120 TC	1.92	396.7	12.21	41	0.13848	−0.34
ModE_05	PERC	60 FC	1.68	328.9	10.44	41.1	0.13982	−0.36
ModF_06	HJT	120 HC	1.84	376.3	10.6	44.5	0.17005	−0.27
ModF_07	HJT	120 HC	1.79	370.5	10.4	44.5	0.16178	−0.27
ModF_08	HJT	120 HC	1.84	371.9	10.8	44.4	0.12736	−0.25
ModF_09	HJT	120 HC	1.84	381.5	10.8	44.4	0.1472	−0.27
ModG_10	IBC	104 FC	1.77	379.7	6.56	75.4	0.12573	−0.30
ModG_11	IBC	104 FC	1.77	391.9	6.52	74.9	0.162	−0.30

[a)]Capital letter in modules names identifies the manufacturer; [b)]all modules have irradiance and wind impact coefficients of $u_0 = 30.1$ and $u_1 = 4.4$, respectively. Except for our reference PV module ($u_0 = 25$ and $u_1 = 6.84$); [c)]number of cells and type: full cell (FC), half cell (HC), third cell (TC); [d)]reference PV module.

© 2023 The Authors. Energy Technology published by Wiley-VCH GmbH

21944296, 0, Downloaded from https://onlinelibrary.wiley.com/doi/10.1002/ente.202300356 by Fraunhofer Ise Inst. Solar Energy Systems, Wiley Online Library on [20/11/2023]. See the Terms and Conditions (https://onlinelibrary.wiley.com/terms-and-conditions) on Wiley Online Library for rules of use; OA articles are governed by the applicable Creative Commons License

characterized by Fraunhofer ISE's module calibration laboratory CalLab PV Modules, which provided input data on spectral responsivity, power rating matrix, angular-loss coefficient (αr), and thermal coefficients (u_0 and u_1), all of which are measured according to IEC 61 853-1 and -2.

All 11 tested PV modules showed standard deviations (STDev) of CSER ranging from 0.57% to 0.75% across most available climate conditions, except for the profiles with higher CSER results (*temperate coastal*, *high elevation*, and *temperate continental*) where the CSER tended to vary more between modules (1.10% and 1.33%). The variation in SSER between data sets in Freiburg was small for all tested modules (STDev of 0.74%). However, the deviations between the *temperate continental* profile and Freiburg were larger, with SSER differences ranging from 1.01% to 3.32% across all tested modules (see **Figure 4**).

It is important to note that the performance of each PV module in each climate profile can differ significantly depending on the module characteristics. For example: 1) PERC modules like ModE_05, ModC_03, and ModB_02 are the modules with the highest CSER results for most climates, except in *subtropical arid*, *tropical humid*, Negev, and Gran Canaria, where their performance decays (with a similar behavior for the reference PV module). These modules do not perform well in climates with high temperatures and irradiance levels, due to their high-temperature coefficient (*TCPmpp*) (up to $-0.36\,\%\,K^{-1}$) and low open-circuit voltage (V_{oc}), which increases their performance dependence on temperature.[10] 2) ModG_10 (IBC) behaves contrary to the previous modules, it has the highest CSER in the profiles *tropical humid*, Negev, and Gran Canaria. This might be attributed to its combination of small *TCPmpp* ($-0.30\,\%\,K^{-1}$), one of the highest V_{oc} within the modules (74.9 V), as well as a low angular loss coefficient (0.12573). 3) ModF modules (HJT) tend to have the lowest performance in this comparison, but ModF_08 (HJT) improves considerably to top positions in the *subtropical arid*, *tropical humid*, *subtropical coastal*, and Negev. This behavior is well correlated with its lowest *TCPmpp* ($-0.25\,\%\,K^{-1}$) and a small angular loss coefficient (0.12736), which gives it the advantage within its technology. However, it presents the worst performance in low light conditions (see Section 4.4), having the highest loss due to irradiance from all the modules in the *temperate coastal* climate, where the highest fraction of low irradiance is found.

4.1. Angular Loss Coefficient Effect

The analysis (results shown in Table S1, Supporting Information) indicates that losses due to AOI from each of the climates range from −1.84% to −3.08% on average across all modules. The *temperate coastal* profile causes the highest losses (averaging −3.08%) and variability (STDev = 0.81%) among the modules. This can be attributed to its largest proportion of diffuse irradiance and highest AOI throughout the year compared to other climates.

The standard IEC61853-3 provides the AOI correction according to the model of Martin and Ruiz through a single empirical coefficient inherent to the PV module called angular loss coefficient (αr).[24] By comparing modules with different αr coefficients in all the different climate profiles, a linear relationship is revealed (**Figure 5**). The modules with the highest angular loss coefficients (e.g., ModF_06 & 07 and ModG_11) exhibit the highest losses ($L_{AOI,year}$) and a high variability in performance within the climates.

4.2. Spectral Response Effect

The effective irradiation available for a specific PV module, after considering angular effects, depends directly on the spectral distribution received and the spectral responsivity of the device. The gain/losses due to spectrum variability range from −1.66% to +3.26% and show wide variability between climates (Table S2, Supporting Information). Only in the *high elevation* climate

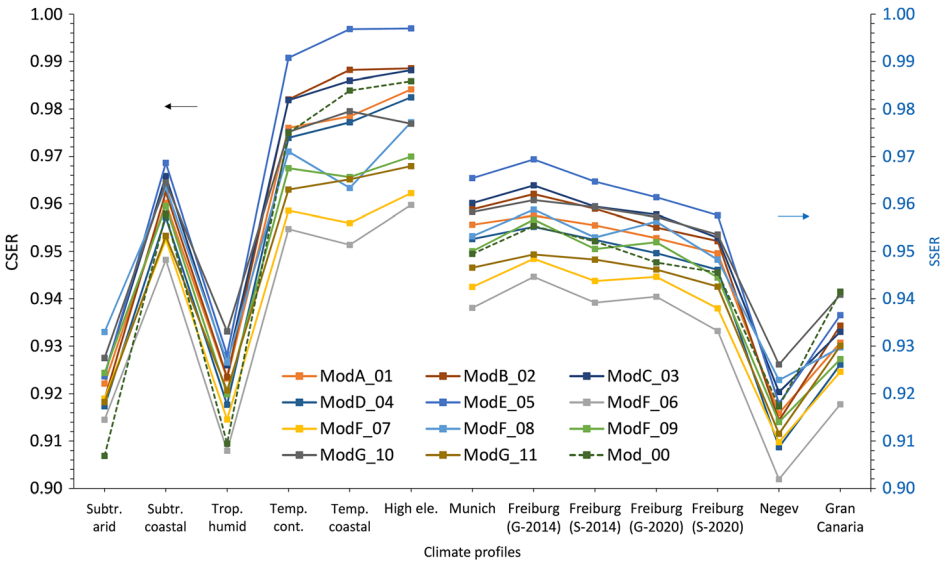

Figure 4. CSER and SSER for 11 monocrystalline silicon PV modules from different manufacturers and our reference PV module from section 2.4. "G" represents ground measurements, while "S" denotes satellite measurements.

© 2023 The Authors. Energy Technology published by Wiley-VCH GmbH

21944296, 0, Downloaded from https://onlinelibrary.wiley.com/doi/10.1002/ente.202300356 by Fraunhofer Ise Inst. Solar Energy Systems, Wiley Online Library on [20/11/2023]. See the Terms and Conditions (https://onlinelibrary.wiley.com/terms-and-conditions) on Wiley Online Library for rules of use; OA articles are governed by the applicable Creative Commons License

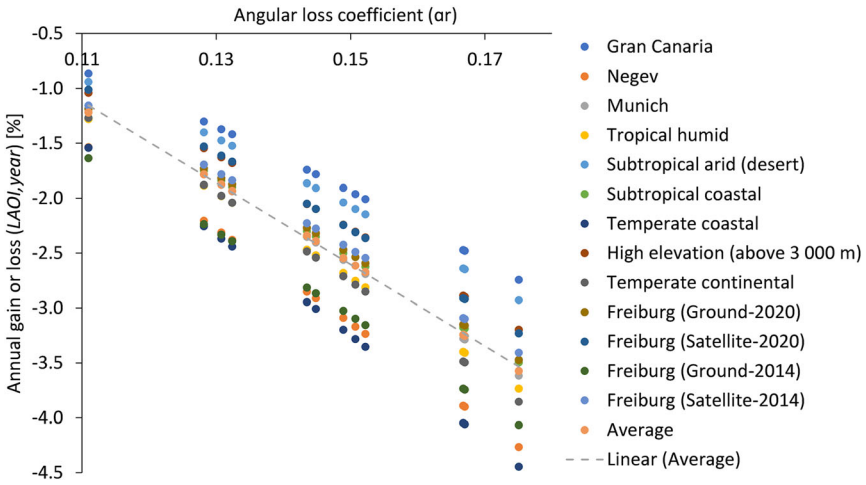

Figure 5. Average annual losses due to AOI for each climate depending on the angular loss coefficient of the tested PV modules.

and in Gran Canaria modules show losses due to spectrum, as reflected by their annual weighted SMM below 1. When comparing ground- and satellite-based climate profiles, the ground-based data sets (Freiburg 2014 and 2020) show higher spectral gains for the modules.[25]

For this study, the tested PV modules have very similar SR curves, as their cell technology is based on monocrystalline silicon. Therefore, the standard deviation between the modules in each climate is small, ranging between 0.04% and 0.49% (Table S2, Supporting Information). Anyhow, the small variability in SR may still show some relationship with the gain or loss for each module. The IBC modules (ModG_10 & 11) have the highest gains compared to the other modules due to their slightly wider SR.

4.3. Influence Due to Temperature Coefficients

The results of the comparison show that there are losses in module performance and higher variability in this effect that are correlated with higher ambient temperatures. The climates with the highest temperatures (*tropical humid*, *subtropical arid*, and Negev) have the highest variability in their effect within the tested modules (STDev from 0.63% to 0.94%) and cause the highest losses (averaging from −4.64% to −5.96%). The climates with average gains due to temperature are the *high elevation* (average gains of 2.99%), *temperate coastal*, and *temperate continental* where the colder temperatures can be found (Figure S4, Supporting Information).

The Faiman model used to estimate the module temperature requires two coefficients (u_0 and u_1) inherent to the PV module, which are determined by standardized measurements of module temperature at different irradiance and wind speed levels.[19] In this study, these coefficients were set to be the same for all 11 PV modules tested, with $u_0 = 30.1$ and $u_1 = 4.4$ obtained from previous measurements to similar modules done in the laboratory CalLab PV Modules.

Another parameter characteristic to each PV module is its power temperature coefficient (*TCPmpp*), which has a strong influence on the module's electrical output (power) with respect to changes in temperature, particularly in those climates where the temperatures are higher. This gives a clear advantage to ModF (HJT) modules with the lowest losses due to temperature. **Figure 6** shows that in temperate climates (*high elevation*, *temperate coastal*, and *temperate continental*), the variation of *TCPmpp* does not majorly affect the gains/losses variation. However, for hotter climates, the design of PV modules with smaller *TCPmpp* might reduce the losses due to temperature significantly.

4.4. Influence Due to PV Module's Low Light Behavior

The efficiency at low irradiance levels leads to a reduction in the energy rating of the PV module, as shown in Table S3, Supporting Information, with averaging losses ranging from −1.03% to −3.41%. The variability in losses within the PV modules in each climate is quite similar, ranging from 0.38% to 0.92%. The *temperate coastal* climate, with 20.9% proportion of low irradiance in POA ($<200\ W^{-2}$), causes the highest variability among modules and the greatest losses, which can be attributed to the high contribution of diffuse light, accordingly also to other studies.[12] Conversely, in climates with high levels of irradiance like *subtropical arid*, *high elevation*, and Negev, modules experience the lowest losses and variability due to this parameter.

Figure 7 illustrates the losses of each module as a function of the proportion of low irradiance in POA ($<200\ W\ m^{-2}$) derived from all the climate profiles. ModE_05, ModB_02, and Mod_00 demonstrate better performance under any proportion of low irradiance, possibly due to their lower level of nominal power compared to the other modules. As expected, a rapid decline and greater losses are observed as the fraction of low irradiance increases. ModF modules (HJT) demonstrate the lowest performance due to low light, particularly ModF_08 in the *temperate coastal* climate.

5. Discussion of Results

The comparison shows that ambient temperature and AOI have the greatest impact on the performance of the PV modules,

© 2023 The Authors. Energy Technology published by Wiley-VCH GmbH

21944296, 0, Downloaded from https://onlinelibrary.wiley.com/doi/10.1002/ente.202300356 by Fraunhofer Ise Inst. Solar Energy Systems, Wiley Online Library on [20/11/2023]. See the Terms and Conditions (https://onlinelibrary.wiley.com/terms-and-conditions) on Wiley Online Library for rules of use; OA articles are governed by the applicable Creative Commons License

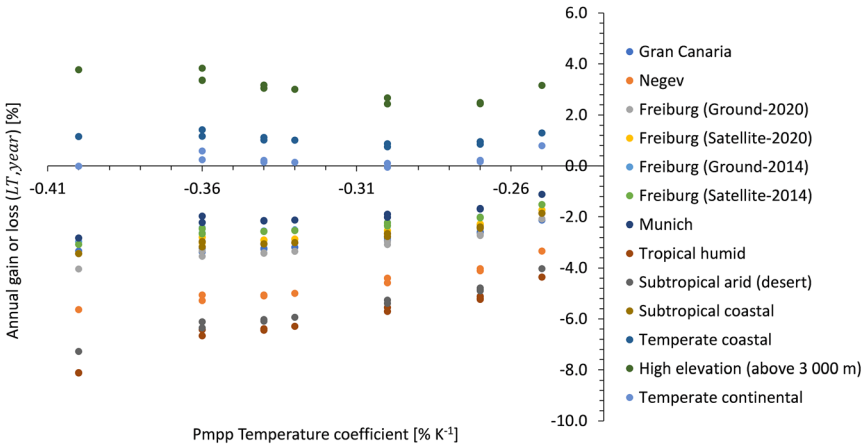

Figure 6. Average annual gain or losses due temperature for each climate profile depending on the PV module's power temperature coefficient (TCPmpp).

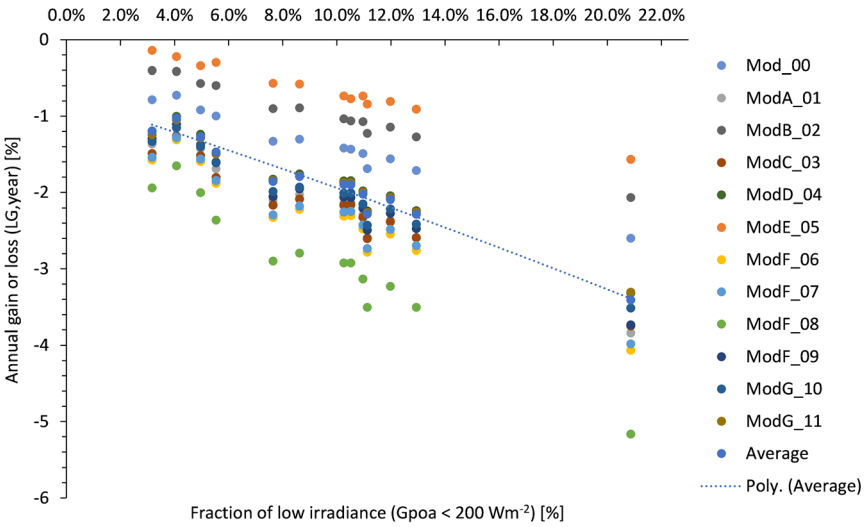

Figure 7. Average annual losses due to irradiance for each tested module depending on the proportion of low irradiance in POA from each of the climate profiles.

particularly in hotter climates like *subtropical arid* as shown in **Figure 8** and Table S4, Supporting Information. Among the modules tested, those with the most resilience to temperature variations are HJT and IBC modules, which have the lowest temperature coefficients. Modules like ModA_01, ModC_03, ModF_08, and ModG_10 exhibit a better response to AOI effects in such climates due to their low angular loss coefficient, which ranges from 0.11 to 0.13.

In temperate climates, like *temperate continental,* shown in Figure 8 and Table S5, Supporting Information, the main influencing parameters are AOI and the irradiance level. In these climates, PERC modules, particularly ModB_02 and ModE_05, with the lowest nominal power in this comparison, show better performance in terms of irradiance levels.

The characteristic angular loss coefficient and power temperature coefficient of the modules exhibit a direct correlation with losses in annual effective irradiation, as seen in Figure 5 and 6, particularly in climates with a high proportion of diffuse irradiance and AOI, such as *temperate coastal,* as well as high ambient temperatures, such as *tropical humid* and *subtropical arid* climates.

The parameters with the greatest influence on the differences between standard and site-specific climate profiles are the variations in spectrum and ambient temperature. Analyzing the gains or losses due to each parameter, we find that: 1) When comparing the *temperate continental* and Freiburg profiles, modules displayed more spectral gains in climates with ground-based data. 2) The comparison between the *temperate continental* and Freiburg also shows considerable differences in ambient temperature. While modules showed gains due to temperature in the *temperate continental,* they exhibited losses in Freiburg profiles.

These differences can cause misleading information on the expected behavior of some modules, such as the case of HJT modules (ModF), which perform better in specific locations like Freiburg due to their better response to temperature variations.

© 2023 The Authors. Energy Technology published by Wiley-VCH GmbH

21944296, 0, Downloaded from https://onlinelibrary.wiley.com/doi/10.1002/ente.202300356 by Fraunhofer Ise Inst. Solar Energy Systems, Wiley Online Library on [20/11/2023]. See the Terms and Conditions (https://onlinelibrary.wiley.com/terms-and-conditions) on Wiley Online Library for rules of use; OA articles are governed by the applicable Creative Commons License

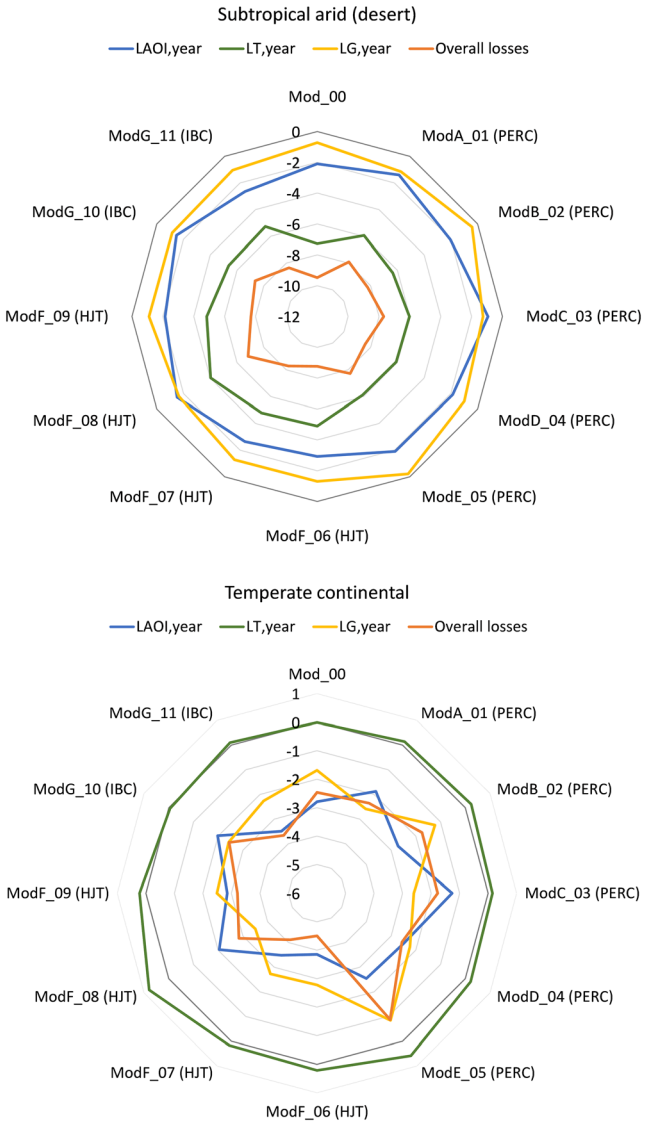

Figure 8. Average annual losses in percentage (%) due to AOI, temperature, and irradiance for each PV module and for the subtropical arid (upper graph) and the temperate continental (lower graph) profile. Spectral gains are omitted in the graphs since there is no significant differences between modules.

6. Conclusions

We explored the feasibility of incorporating site-specific climate profiles into energy rating calculations by comparing the data sets provided in IEC 61 853-4 with monitoring locations in Freiburg, Gran Canaria, and Negev. A detailed comparison of the parameters affecting the CSER, including angular, spectral, temperature, and irradiance effects, provided insights into the differences between the climate profiles and allowed us to answer our primary question regarding the representativeness of the standard regions for South/Central Europe.

We found that year-to-year variability in climate conditions and differences between ground- and satellite-based data had a small impact on the CSER for all tested modules in Freiburg. In contrast, the deviations between the respective standard profile and Freiburg were more significant, with SSER deviations to CSER ranging from 1.01% to 3.32% across all tested modules. The solar spectrum and ambient temperature were the main parameters that cause these differences. The deviations are found to be larger than the known uncertainties of CSER due to module measurements of some 2% where it has been concluded that the greater contribution to uncertainty is from the measurement of the power matrix and modeling of module temperature.[1,24] Therefore, we recommend the use of a site-specific data set in this region when a more detail benchmarking analysis is required, as suggested by Ref. [1] with the South/Central Europe location (Munich).

Deviations in SSER for all modules in this study range from 1.64% to 3.38% for Gran Canaria compared to the *subtropical coastal* profile, whereas for Negev compared to the *subtropical arid* profile, the deviations in SSER were smaller, between 0.13% and 1.26%. The parameter that had the greatest influence was the variation in the solar spectrum, with an average difference in spectral losses from all the modules of 3.85% between Gran Canaria and the *subtropical coastal* profile. However, further validation of these differences is necessary using more years of data and spectroradiometers with a wider wavelength range.

Based on the analysis of differences between ground- and satellite-based climate data sets for our location in Freiburg, we observed that the largest differences were in the solar spectrum, with the ground-based climate profiles showing higher spectral gains (ranging from 0.99% to 1.6% for all tested modules). Our findings suggest that the deviations were primarily caused by differences in atmosphere characterization between the ground-based and satellite-based data. As per Ref. [23], this could be due to the satellite-based data using mean values or low temporal resolution for parameters such as aerosol-optical depth and water vapor content. The use of monthly climatologies with constant rural aerosol type in the satellite-based data could also contribute to the deviations.

The benchmarking study conducted on monocrystalline silicon PV modules from various manufacturers revealed the impact of modules characteristics on the CSER results. Comparison of climate profiles has identified the parameters with greatest impact in the CSER are the reflectivity as function of AOI variations and the ambient temperature in hot climates, and the AOI and irradiance level in temperate climates. The most challenging conditions for c-Si modules are found in the *temperate coastal* climate with a high proportion of diffuse irradiance and AOI, as well as in the *tropical humid* and *subtropical arid* climates with high ambient temperatures. It is crucial to understand the module response to each influencing parameter and fitting modules with appropriate characteristics, such as angular loss coefficient, low light behavior, and power temperature coefficient, which can lead to significant improvements. Taking the general overview of CSER results on the six standard regions might mislead on the module's real behavior and performance ranking in benchmarking comparisons.

We noticed a high variability in CSER between modules in the *temperate continental*, *temperate coastal*, and *high elevation* climates. The parameters that influence these variations were the ambient temperature and irradiance levels. Furthermore,

© 2023 The Authors. Energy Technology published by Wiley-VCH GmbH

21944296, 0, Downloaded from https://onlinelibrary.wiley.com/doi/10.1002/ente.202300356 by Fraunhofer Ise inst. Solar Energy Systems, Wiley Online Library on [20/11/2023]. See the Terms and Conditions (https://onlinelibrary.wiley.com/terms-and-conditions) on Wiley Online Library for rules of use; OA articles are governed by the applicable Creative Commons License

in the *temperate coastal* and *temperate continental*, the CSER might also vary the most due the AOI effects.

The study has been limited by the available cell technologies. Including modules with different spectral responsivities might provide more insight into the spectral response effect. Further, we will validate our results with outdoor measurements of some of the modules presented in this study.

Supporting Information

Supporting Information is available from the Wiley Online Library or from the author.

Acknowledgements

M.R. is thankful for the financial support of Nagelschneider Foundation (Munich, Germany). Authors appreciate data provided by the German Weather Service (Deutscher Wetterdienst—DWD) through their EUMETSAT's Satellite Application Facility on Climate Monitoring (CM SAF).

Open Access funding enabled and organized by Projekt DEAL.

Conflict of Interest

The authors declare no conflict of interest.

Data Availability Statement

The data that support the findings of this study are available from the corresponding author upon reasonable request.

Keywords

benchmarking, climate profiles, energy rating, spectral irradiance

Received: March 31, 2023
Revised: May 30, 2023
Published online:

[1] T. Huld, E. Salis, A. Pozza, W. Herrmann, H. Müllejans, *Sol. Energy* **2016**, *133*, 349.
[2] D. Dirnberger, B. Müller, C. Reise, *Prog. Photovoltaics Res. Appl.* **2015**, *23*, 1754.
[3] T. Huld, A. Amillo, *Energies* **2015**, *8*, 5159.
[4] International Electrotechnical Commission (IEC), IEC 61853-4 Photovoltaic (PV) Module Performance Testing and Energy Rating — Part 4: Standard Reference Climatic Profiles, **2018**, Geneva, Switzerland.
[5] International Electrotechnical Commission (IEC), IEC 61853-1 Photovoltaic (PV) Module Performance Testing and Energy Rating — Part 1: Irradiance And Temperature Performance Measurements and Power Rating, **2011**, Geneva, Switzerland.
[6] International Electrotechnical Commission (IEC), IEC 61853-2 Photovoltaic (PV) Module Performance Testing and Energy Rating — Part 2: Spectral Responsivity, Incidence Angle and Module Operating Temperature Measurements Rating, **2016**, Geneva, Switzerland.
[7] T. Huld, E. Dunlop, H. G. Beyer, R. Gottschalg, *Sol. Energy* **2013**, *93*, 267.
[8] A. Amillo, T. Huld, P. Vourlioti, R. Müller, M. Norton, *Energies* **2015**, *8*, 3455.
[9] T. Behrendt, J. Kühnert, A. Hammer, E. Lorenz, J. Betcke, D. Heinemann, *25th European Photovoltaic Solar Energy Conference and Exhibition*, Valencia, Spain 6–10 September **2010**.
[10] C. Monokroussos, Y. Zhang, E. W. Lee, F. Xu, A. Zhou, Y. Zhang, W. Herrmann, *EPJ Photovoltaics* **2023**, *14*, 6.
[11] B. Bora, R. Kumar, O. S. Sastry, B. Prasad, S. Mondal, A. K. Tripathi, *Sol. Energy* **2018**, *174*, 901.
[12] C. Monokroussos, X. Y. Zhang, M. Schweiger, D. Etienne, C. Zou, *EPJ Photovoltaics* **2017**, *14*, 6.
[13] W. F. Holmgren, C. W. Hansen, M. A. Mikofski, *JOSS* **2018**, *3*, 884.
[14] T. M. Klucher, *Sol. Energy* **1979**, *23*, 111.
[15] D. G. Erbs, S. A. Klein, J. A. Duffie, *Sol.Energy* **1982**, *28*, 293.
[16] J. Schulz, P. Albert, H.-D. Behr, D. Caprion, H. Deneke, S. Dewitte, B. Dürr, P. Fuchs, A. Gratzki, P. Hechler, R. Hollmann, S. Johnston, K.-G. Karlsson, T. Manninen, R. Müller, M. Reuter, A. Riihelä, R. Roebeling, N. Selbach, A. Tetzlaff, W. Thomas, M. Werscheck, E. Wolters, A. Zelenka, *Atmos. Chem. Phys.* **2009**, *9*, 1687.
[17] M. Ruben Vogt, S. Riechelmann, A. M. Gracia-Amillo, A. Driesse, A. Kokka, K. Maham, P. Karha, R. Kenny, C. Schinke, K. Bothe, J. Blakesley, E. Music, F. Plag, G. Friesen, G. Corbellini, N. Riedel-Lyngskar, R. Valckenborg, M. Schweiger, W. Herrmann, *IEEE J. Photovoltaics* **2022**, *12*, 844.
[18] A. Driesse, "PV Performance Labs Tools for Python", https://github.com/adriesse/pvpltools-python, **2020**.
[19] International Electrotechnical Commission (IEC), IEC 61853-3 Photovoltaic (PV) Module Performance Testing and Energy Rating — Part 3: Energy Rating of PV Modules, **2018**, Geneva, Switzerland.
[20] International Electrotechnical Commission (IEC), IEC 60904-7 Photovoltaic Devices - Part 7: Computation of the Spectral Mismatch Correction For Measurements of Photovoltaic Devices, **2019**, Geneva, Switzerland.
[21] D. Dirnberger, G. Blackburn, B. Müller, C. Reise, *Sol. Energy Mater. Sol. Cells* **2015**, *132*, 431.
[22] International Electrotechnical Commission (IEC), IEC 60904-3 Photovoltaic Devices - Part 3: Measurement Principles for Terrestrial Photovoltaic (PV) Solar Devices with Reference Spectral Irradiance Datamodules, **2019**, Geneva, Switzerland.
[23] T. Behrendt, J. Kuehnert, A. Hammer, E. Lorenz, J. Betcke, D. Heinemann, *Sol. Energy* **2013**, *98*, 100.
[24] N. Martin, J. M. Ruiz, *Sol. Energy Mater. Sol. Cells* **2001**, *70*, 25.
[25] R. Mueller, T. Behrendt, A. Hammer, A. Kemper, *Remote Sens.* **2012**, *4*, 622.

© 2023 The Authors. Energy Technology published by Wiley-VCH GmbH

21944296, 0, Downloaded from https://onlinelibrary.wiley.com/doi/10.1002/ente.202300356 by Fraunhofer Ise Inst. Solar Energy Systems, Wiley Online Library on [20/11/2023]. See the Terms and Conditions (https://onlinelibrary.wiley.com/terms-and-conditions) on Wiley Online Library for rules of use; OA articles are governed by the applicable Creative Commons License